



## Diffusion-thermo effects on MHD free convective radiative and chemically reactive boundary layer flow through a porous medium over a vertical plate

J. Prakash<sup>a,\*</sup>, P. Durga Prasad<sup>b</sup>, R. V. M. S. S. Kiran Kumar<sup>c</sup> and S. V. K. Varma<sup>d</sup>

<sup>a</sup> Department of Mathematics, University of Botswana, Private Bag 0022, Gaborone, Botswana

<sup>b, c, d</sup> Department of Mathematics, Sri Venkateswara University, Tirupati – 517502, A. P., India

---

### Article info:

Received: 01/10/2015

Accepted: 18/01/2016

Online: 03/03/2016

---

### Keywords:

Diffusion-thermo effect,  
Thermal radiation,  
Chemical reaction,  
Magnetic fields.

### Abstract

The main purpose of this work is to investigate the porous medium and diffusion-thermo effects on unsteady combined convection magneto hydrodynamics boundary layer flow of viscous electrically conducting fluid over a vertical permeable surface embedded in a high porous medium, in the presence of first order chemical reaction and thermal radiation. The slip boundary condition is applied at the porous interface. A uniform Magnetic field is applied normal to the direction of the fluid flow. The non-linear coupled partial differential equation are solved by perturbation method and obtained the expressions for concentration, temperature and velocity fields. The rate of mass transfer in terms of Sherwood number  $h$ , the rate of heat transfer in terms of Nusselt number  $Nu$  and the Skin friction coefficient  $Cf$  are also derived. The Profiles of fluid flow quantities for various values of physical parameters are presented and analyzed. Profiles of fluid flow quantities for various values of physical parameters are presented and analyzed.

---

### Nomenclature

$A$	Suction velocity parameter
$B_0$	Magnetic field of uniform strength
$C$	Species concentration
$C^*$	Dimensional concentration
$C_p$	Specific heat at constant pressure
$C_s$	Concentration susceptibility
$C_w$	Species concentration at the plate
$C_\infty$	Species concentration far away from the plate
$Cf$	Skin friction coefficient
$D$	Molecular diffusivity
$e_{b\lambda}$	Planck's function
$g$	Acceleration due to gravity

$Gm$	Solutal Grashof number
$Gr$	Thermal Grashoff number
$K$	Permeability parameter
$D_m$	Coefficient of mass diffusivity
$K^*$	Permeability of the porous medium
$K_T$	Thermal diffusion ratio
$K_{\lambda w}$	Absorption coefficient at the wall
$M$	Magnetic field parameter
$F$	Radiation parameter
$Nu$	Nusselt number
$n^*$	Constant
$P^*$	Pressure
$Pr$	Prandtl number
$Q$	Heat source/sink parameter
$Q^*$	Sink strength

---

\* corresponding author

Email address: prakashj@mopipi.ub.bw

$Q_0$	Dimensional heat absorption coefficient
$Q_1$	Absorption of radiation parameter
$Q_l^*$	Coefficient of proportionality for the absorption
$q_r^*$	Radiative heat flux
$Sc$	Schmidt number
$Sh$	Sherwood number
$T$	Fluid Temperature
$T^*$	Temperature of the fluid near the plate
$T_w$	Temperature at the wall
$T_\infty$	Temperature far away from the plate
$u^*, v^*$	Components of dimensional velocities
$u^*$	Velocity of the fluid along $x^*$
$U_\infty^*$	Free stream dimensional velocity
$U_p$	Wall dimensional velocity
$v^*$	Velocity of the fluid along $y^*$
$U_0$	Scale of free stream velocity
$V_0$	Section velocity
$C_p$	Specific heat at constant pressure
$C_v$	Specific heat at constant volume
$x^*, y^*$	Dimensional distances along and perpendicular to the plate
$Re_x$	Local Reynolds number

**Greek symbols**

	Fluid dynamic viscosity
$\alpha$	Fluid thermal diffusivity
$\nu$	Coefficient of kinematic viscosity
$\beta$	Coefficient of volumetric expansion for the heat transfer
$\beta^*$	Coefficient of volumetric expansion for the fluid
$\beta_0$	Magnetic field coefficient
$\beta_T, \beta_c$	Thermal and concentration expansion coefficients
$\rho$	Density of the fluid
$\sigma$	Electrically conductivity of the fluid
$\eta$	Dimensionless normal distance
$\emptyset$	Heat source parameter
$\emptyset_1$	Porous permeability parameter
$\kappa$	Thermal conductivity

**Superscripts**

'	Differentiation with respect to $y$
*	Dimensional properties

**Subscripts**

p	Plate
w	Wall condition
$\infty$	Free stream condition

---

**1. Introduction**

Fluid currents formed in a fluid-saturated porous medium during convective heat transfer have many important applications, such as oil and gas production, central grain storage, porous insulation, and geothermal energy. The study of natural convection through a porous medium also throws some light on the influence of environment such as temperature and pressure on the germination of seeds. In many situations, heat and mass transfer on the hydromagnetic flow near the vertical plate is encountered, e.g. the cooling of nuclear reactor using electrically conducting coolants such as liquid sodium and mercury, studied by Rath and Prida [1]. Raptis [2] and also Jha and Prasad [3] have studied the steady free convection flow and mass transfer through a porous medium bounded by an infinite vertical plate for the flow near the plate using Yamamoto and Iwamura's [4] model. Gebhart and Pera [5] studied the laminar flows which arise in fluids due to the interaction of the force of gravity and density differences caused by the simultaneous diffusion of thermal energy and chemical species.

As stated by Pal and Talukdar [6], convection in porous media has gained significant attention in recent years because of its importance in engineering applications such as solid matrix heat exchangers, geothermal systems, thermal insulations, oil extraction, and storage of nuclear waste materials. Convection in porous media is also applied to underground coal gasification, ground water hydrology, iron blast furnaces, wall cooled catalytic reactors, solar power collectors, energy efficient drying processes, cooling of electronic equipment, and natural convection in the earth's crust. Reviews of the applications associated with convective flows in porous media can be found in Nield and Bejan's [7] work. The fundamental problems of flow through and past porous media have been studied extensively over the years both theoretically and experimentally by Cheng [8] and Rudraiah [9]. The effect of Beavers-Joseph slip velocity and transverse magnetic field on an electrically conducting viscous fluid in a horizontal channel bounded

on both sides of the porous substrates of finite thickness was studied by Rudraiah et al. [10], which is equivalent to the problem of forced convection, in which the momentum equation is independent from concentration distribution and the diffusion equation is coupled with the velocity distribution using Beavers-Joseph slip condition at the porous interface.

In many chemical engineering processes, a chemical reaction occurs between a foreign mass and the fluid in which the plate is moving. These processes take place in numerous industrial applications, e.g. manufacturing of ceramics or glassware, polymer production, and food processing. Chemical reactions can be codified as either homogeneous or heterogeneous processes, which depends on whether they occur at an interface or as a single-phase volume reaction. Many transport processes exist in mass transfer in nature as a result of combined buoyancy effects of thermal diffusion and diffusion of chemical species. Apelblat [11] studied an analytical solution for mass transfer by a first order chemical reaction. Das et al. [12] analyzed the effects of homogeneous first order chemical reaction on the flow passing an impulsively started infinite vertical plate with uniform heat flux and mass transfer. Chambre and Young [13] analyzed a first order chemical reaction in the neighborhood of a horizontal plate.

Radiative convective flows are encountered in various ways in the environment, e.g. heating and cooling chambers, evaporation from large open water reservoirs, fossil fuel combustion energy processes, solar power technology, astrophysical flows, and space vehicle re-entry. Radiative heat and mass transfer plays an important role in manufacturing industries for the design of reliable equipment. Nuclear power plants, gas turbines, and various propulsion devices for satellites, missiles, aircraft, and various space vehicles are the examples of such engineering applications. If the temperature of the surrounding fluid is rather high, radiation effects play an important role, a situation that exists in space technology. In such cases, one has to take into account the effects of thermal radiation and mass diffusion.

The thermal radiation effects of an optically thin gray gas bounded by a stationary vertical plate was studied by England and Emery [14]. The radiative natural convective flow of an optically thin gray-gas past a semi-infinite vertical plate was considered by Soundalgekar and Takhar [15]. In all of the above studies, the stationary vertical plate has been considered. The effects of the thermal radiation and free convection flow past a moving vertical plate studied by Raptis and Perdakis [16]. Ibrahim et al. [17] recently reported computational solutions for transient reactive magneto hydrodynamic heat transfer with heat source and wall flux effects. They have also analyzed the effects of the chemical reaction and radiation absorption on the unsteady MHD free convection flow past a semi-infinite vertical permeable moving plate with heat source and suction. Due to the importance of Soret (thermal-diffusion) and Dufour (diffusion thermo) effects for the fluids with very light molecular weight as well as medium molecular weight many investigators have studied and reported results for these flows of whom the names are Dursunkaya and Worek [18], Anghel *et al.* [19], Postelnicu [20] are worth mentioning.

Chamkha[21] investigated unsteady convective heat and mass transfer past a semi-infinite porous moving plate with heat absorption. Chamkha[22] studied the MHD flow of a numerical of uniformly stretched vertical permeable surface in the presence of heat generation/absorption and a chemical reaction. Mohamed [23] has discussed double diffusive convection radiation interaction on unsteady MHD flow over a vertical moving porous plate with heat generation and Soret effects. Muthucumaraswamy and Janakiraman[24] studied MHD and radiation effects on moving isothermal vertical plate with variable mass diffusion. Rajesh and Varma[25] studied thermal diffusion and radiation effects on MHD flow past a vertical plate with variable temperature. Kumar and Varma[26] investigated thermal radiation and mass transfer effects on MHD flow past an impulsively started exponentially accelerated vertical plate with variable temperature and mass diffusion.

Raptis et al.[27] studied the hydromagnetic free convection flow of an optically thin gray gas taking into account the induced magnetic field in the presence of radiation and the analytical solutions were obtained by perturbation technique. Orhan and Ahmad [28] examined MHD mixed convective heat transfer along a permeable vertical infinite plate in the presence of radiation and solutions are derived using Keller box scheme and accurate finite-difference scheme. Ahmed [29] investigated the study of influence of thermal radiation and magnetic Prandtl number on the steady MHD heat and mass transfer mixed convection flow of a viscous, incompressible, electrically-conducting Newtonian fluid over a vertical porous plate with induced magnetic field.

When heat and mass transfer occur simultaneously in moving fluid, the relations between the fluxes and the driving potentials are of a more intricate nature. It has been observed that an energy flux can be generated not only by temperature gradients but also by concentration gradients. The energy flux caused by a concentration gradient is termed the diffusion-thermo (Dufour) effect. In most of the studies related to heat and mass transfer process, Soret and Dufour effects are neglected on the basis that they are of a smaller order of magnitude than the effects described by Fourier's and Fick's laws. But these effects are considered as second order phenomena and may become significant in areas such as hydrology, petrology, geosciences, etc. For fluids with medium molecular weight ( $H_2$ , air), Dufour and Soret effects should not be neglected as indicated by Eckert and Drake [30]. Prakash et al. [31] analyzed Diffusion-Thermo and Radiation Effects on Unsteady MHD Flow through Porous Medium Past an Impulsively Started Infinite Vertical Plate with Variable Temperature and Mass Diffusion. To our best knowledge, the interaction between the diffusion-thermo and chemical reaction in the presence of porous medium, heat absorption/generation, thermal radiation, radiation absorption effects has received little attention. Hence, an attempt is made to study the diffusion-thermo effects on an unsteady MHD free convective heat and mass transfer

flow of a viscous incompressible electrically conducting fluid through porous medium from a vertical porous plate with varying suction velocity in slip flow regime.

To the best of our knowledge, the interaction between the diffusion-thermo and chemical reaction in the presence of porous medium, heat absorption/generation, thermal radiation, radiation absorption effects has received little attention. Hence, an attempt is made to study the diffusion-thermo effects on an unsteady MHD free convective heat and mass transfer flow of a viscous incompressible electrically conducting fluid through porous medium from a vertical porous plate with varying suction velocity in slip flow regime.

## 2. Mathematical formulation

Consider an unsteady two dimensional flow of an incompressible viscous, electrically conducting, and heat absorbing fluid past a semi-infinite vertical permeable plate embedded in a uniform porous medium and subjected to a uniform transverse magnetic field in the presence of thermal and concentration buoyancy effects. The applied magnetic field is also taken as being weak so that Hall and ion slip effects may be neglected. We assume that the Dufour effects may be described by a second order concentration derivative with respect to the transverse coordinate in the energy equation. Further to our assumption that there is no applied voltage which implies the absence of an electric field. The plate is maintained at constant temperature  $T_w$  and concentration  $C_w$ , which is higher than the ambient temperature  $T_\infty$  and concentration  $C_\infty$ , respectively. The chemical reactions take place in the flow and all thermo physical properties are assumed to be constant. Due to the semi-infinite plane surface assumption, the flow variables are the functions of  $y^*$  and time  $t^*$  only. Under the usual boundary layer approximations, the equations are governed by the following equations:

$$\frac{\partial v^*}{\partial y^*} = 0 \tag{1}$$

$$\frac{\partial u^*}{\partial t^*} + v^* \frac{\partial u^*}{\partial y^*} = -\frac{1}{\rho} \frac{\partial p^*}{\partial x^*} + v \frac{\partial^2 u^*}{\partial y^{*2}} - \frac{\sigma B_0^2}{\rho} u^* + g\beta_T(T^* - T_\infty) + g\beta_c(C^* - C_\infty) - \frac{v}{K^*} u^* \quad (2)$$

$$\frac{\partial T^*}{\partial t^*} + v^* \frac{\partial T^*}{\partial y^*} = \frac{K}{\rho C_p} \frac{\partial^2 T^*}{\partial y^{*2}} - \frac{1}{\rho C_p} \frac{\partial q_r^*}{\partial y^*} - \frac{Q_0}{\rho C_p} (T^* - T_\infty) + \frac{Q_1^*}{\rho C_p} (C^* - C_\infty) + \frac{D_m K_T}{C_s \rho C_p} \frac{\partial^2 C^*}{\partial y^{*2}} \quad (3)$$

$$\frac{\partial C^*}{\partial t^*} + v^* \frac{\partial C^*}{\partial y^*} = D \frac{\partial^2 C^*}{\partial y^{*2}} - R(C^* - C_\infty) \quad (4)$$

where  $x^*$ ,  $y^*$ , and  $t^*$  are the dimensional distances along  $x^*$  and  $y^*$  directions and dimensional time, respectively,  $u^*$  and  $v^*$  are the components of dimensional velocities along  $x^*$  and  $y^*$  directions, respectively,  $T^*$  is the dimensional temperature,  $C^*$  is the dimensional concentration,  $T_w$  and  $C_w$  are the temperature and concentration at the wall,  $C_\infty$  and  $T_\infty$  are the free stream dimensional concentration and temperature,  $\rho$  is the density,  $\nu$  is kinematic viscosity,  $C_p$  is the specific heat at constant pressure,  $\sigma$  is the fluid electrical conductivity,  $B_0$  is the magnetic induction,  $K^*$  is the permeability of the porous medium,  $q_r^*$  is radiative heat flux,  $Q_0$  is the dimensional heat absorption coefficient,  $Q_1^*$  is the coefficient of proportionality for the absorption,  $R$  is the chemical reaction,  $\beta_T$  and  $\beta_c$  are the thermal and concentration expansion coefficients,  $D$  is the molecular diffusivity,  $D_m$  is the coefficient of mass diffusivity,  $K_T$  is the thermal diffusion ratio,  $Q_0(T^* - T_\infty)$  is assumed to be the amount of heat generated or absorbed per unit volume, and  $Q_0$  is a constant.

The radiative heat flux is considered, which has been given by Cogley et al. [32] as well as Pal and Talukdar [6] as:

$$\frac{\partial q_r^*}{\partial y^*} = 4(T^* - T_\infty)I' \quad (5)$$

where  $I' = \int_0^\infty K_{\lambda w} \frac{\partial e_{b\lambda}}{\partial T^*} d\lambda$ ,  $K_{\lambda w}$  is the coefficient of absorption near the wall and  $e_{b\lambda}$  is Planck's function.

Under the above-stated assumption, the initial and boundary conditions for the velocity distribution involving slip flow, temperature, and concentration distributions are defined as:

$$u^* = u_{slip}^* = \frac{\sqrt{k} \partial u^*}{\alpha \partial y^*}, T^* = T_w + \epsilon(T_w - T_\infty)e^{n^*t^*} \text{ at } y^* = 0 \quad (6)$$

$$C^* = C_w + \epsilon(C_w - C_\infty)e^{n^*t^*} \text{ at } y^* = 0 \quad (7)$$

$$u^* = U_\infty^* = U_0(1 + \epsilon e^{n^*t^*}), T^* \rightarrow T_\infty, C^* \rightarrow C_\infty \text{ as } y^* \rightarrow \infty \quad (8)$$

From Eq. (1) it is clear that the suction velocity at the plate surface is either constant or a function of time only. Hence, it is assumed that

$$v^* = -V_0(1 + \epsilon A e^{n^*t^*}) \quad (9)$$

where  $V_0$  is the mean suction velocity and  $\epsilon A \ll 1$ . The negative sign indicated that the suction velocity is directed towards the plate. In the free stream Eq.(2) gives

$$-\frac{1}{\rho} \frac{dp^*}{dx^*} = \frac{dU_\infty^*}{dt^*} + \frac{\sigma}{\rho} B_0^2 U_\infty^* + \frac{\nu}{K^*} U_\infty^* \quad (10)$$

On introducing the non-dimensional quantities:

$$\begin{aligned} u = \frac{u^*}{U_0}, \vartheta = \frac{\vartheta^*}{V_0}, y = \frac{v_0 y^*}{\nu}, U_\infty = \frac{U_\infty^*}{U_0}, t = \frac{V_0^2 t^*}{\nu}, \\ \theta = \frac{T^* - T_\infty}{T_w - T_\infty}, C = \frac{C^* - C_\infty}{C_w - C_\infty}, n = \frac{n^* \nu}{V_0^2} \\ Gr = \frac{\rho g \nu (T_w - T_\infty) \beta_T}{U_0 V_0^2}, \\ Gm = \frac{\rho g \nu (C_w - C_\infty) \beta_c}{U_0 V_0^2}, M = \frac{\sigma \nu B_0^2}{\rho V_0^2}, Pr = \frac{\nu C_p}{K}, \phi = \frac{Q_0 \nu}{\rho V_0^2 C_p}, \\ Q_1 = \frac{Q_1^* \nu (C_w - C_\infty)}{V_0^2 (T_w - T_\infty)}, F = \frac{4\nu I'}{V_0^2 \rho C_p}, Sc = \frac{\nu}{D}, \gamma = \frac{R\nu}{V_0^2}, \\ Du = \frac{D_m k_T (C_w - C_\infty)}{C_s K (T_w - T_\infty)}, K = \frac{V_0^2 K^*}{\nu^2}. \end{aligned} \quad (11)$$

Considering the above dimensionless variables, the basic field of Eqs. (2) through (4) can be expressed in a dimensionless form as:

$$\frac{\partial u}{\partial t} - (1 + \epsilon A e^{nt}) \frac{\partial u}{\partial y} = \frac{dU_\infty}{dt} + M_1(U_\infty - U) + \frac{\partial^2 u}{\partial y^2} + Gr\theta + GmC, \quad (12)$$

$$\frac{\partial \theta}{\partial t} - (1 + \epsilon Ae^{nt}) \frac{\partial \theta}{\partial y} = \frac{1}{Pr} \frac{\partial^2 \theta}{\partial y^2} - F\theta + Q_1 C - \Phi \theta + \frac{Du}{Pr} \left( \frac{\partial^2 C}{\partial y^2} \right) \quad (13)$$

$$\frac{\partial C}{\partial t} - (1 + \epsilon Ae^{nt}) \frac{\partial C}{\partial y} = \frac{1}{Sc} \frac{\partial^2 C}{\partial y^2} - \gamma C \quad (14)$$

The corresponding initial and boundary conditions in Eqs. (6)-(8) in a non-dimensional form are given below:

$$u = u_{slip} = \Phi_1 \frac{\partial u}{\partial y}, \theta = 1 + \epsilon e^{nt}, C = 1 + \epsilon e^{nt} \text{ at } y = 0 \quad (15)$$

$$U \rightarrow U_\infty = (1 + \epsilon e^{nt}), \theta \rightarrow 0, C \rightarrow 0 \text{ as } y \rightarrow \infty \quad (16)$$

where  $\Phi_1 = \frac{\sqrt{k} U_0 V_0}{\alpha v}$  is the porous permeability parameter.

### 3. Method of solution

The Eqs. (12) - (14) are coupled non-linear partial differential equations whose solutions in closed-form are difficult to obtain. To solve these coupled non-linear partial differential equations, we assume that the unsteady flow is superimposed on the mean steady flow, so that in the neighborhood of the plate, we have

$$u = f_0(y) + \epsilon e^{nt} f_1(y) + O(\epsilon^2) \quad (17)$$

$$\theta = g_0(y) + \epsilon e^{nt} g_1(y) + O(\epsilon^2) \quad (18)$$

$$C = h_0(y) + \epsilon e^{nt} h_1(y) + O(\epsilon^2) \quad (19)$$

By substituting the set of Eqs. (17) - (19) into Eqs. (12) - (14) and equating the harmonic and non-harmonic terms, and neglecting the higher order terms in  $\epsilon$ , we obtain

$$f_0'' + f_0' - M_1 f_0 = -M_1 - Gr g_0 - Gm h_0 \quad (20)$$

$$f_1'' + f_1' - (M_1 + n) f_1 = -(M_1 + n) - A f_0' - Gr g_1 - Gm h_1 \quad (21)$$

$$g_0'' + Pr g_0' - Pr (F + \Phi) g_0 = -Pr Q_1 h_0 - Duh_0'' \quad (22)$$

$$g_1'' + Pr g_1' - Pr (F + \Phi + n) g_1 = -Pr Q_1 h_1 - Duh_1'' - Pr A g_0' \quad (23)$$

$$h_0'' + Sch_0' - Sc \gamma h_0 = 0 \quad (24)$$

$$h_1'' + Sch_1' - Sc(\gamma + n) h_1 = -ASch_0' \quad (25)$$

where the prime denotes the differentiation with respect to  $y$ . Now, the corresponding boundary conditions are:

$$f_0 = \Phi_1 f_0', f_1 = \Phi_1 f_1', g_0 = 1, h_1 = 1, h_0 = 1, h_1 = 1 \text{ at } y = 0 \quad (26)$$

$$f_0 = 1, f_1 = 1, g_0 \rightarrow 0, g_1 \rightarrow 0, h_0 \rightarrow 0, h_1 \rightarrow 0 \text{ as } y \rightarrow \infty. \quad (27)$$

By solving the set of Eqs. (20) - (25) using boundary conditions (26) - (27), the following set of solutions is obtained:

$$f_0 = 1 + B_4 e^{-m_6 y} - A_3 e^{-m_2 y} - A_2 e^{-P_1 y} \quad (28)$$

$$f_1 = 1 + B_5 e^{-m_3 y} + A_4 e^{-m_6 y} - A_{10} e^{-m_2 y} - B_1 e^{-P_1 y} - B_2 e^{-m_5 y} - B_3 e^{-m_4 y} \quad (29)$$

$$g_0 = (1 - A_1) e^{-m_2 y} + A_1 e^{-P_1 y} \quad (30)$$

$$g_1 = A_9 e^{-m_5 y} + A_6 e^{-P_1 y} + A_7 e^{-m_2 y} + A_8 e^{-m_4 y} \quad (31)$$

$$h_0 = e^{-P_1 y} \quad (32)$$

$$h_1 = (1 - A_5) e^{-m_4 y} + A_5 e^{-P_1 y} \quad (33)$$

$$u(y, t) = 1 + B_4 e^{-m_6 y} - A_3 e^{-m_2 y} - A_2 e^{-P_1 y} + \epsilon e^{nt} (1 + B_5 e^{-m_3 y} + A_4 e^{-m_6 y} - A_{10} e^{-m_2 y} - B_1 e^{-P_1 y} - B_2 e^{-m_5 y} - B_3 e^{-m_4 y}) \quad (34)$$

$$\theta(y, t) = (1 - A_1) e^{-m_2 y} + A_1 e^{-P_1 y} + \epsilon e^{nt} (A_9 e^{-m_5 y} + A_6 e^{-P_1 y} + A_7 e^{-m_2 y} + A_8 e^{-m_4 y}) \quad (35)$$

$$C(y, t) = e^{-P_1 y} + \epsilon e^{nt} ((1 - A_5) e^{-m_4 y} + A_5 e^{-P_1 y}) \quad (36)$$

The coefficient of Skin-friction, rate of heat transfer in terms of Nusselt number, and rate of mass transfer are the important physical parameters for this kind of boundary layer flow. Hence, these quantities are defined and derived as follows:

$$C_{fx} = \frac{\tau_w}{\rho U_0 V_0} = \left(\frac{\partial u}{\partial y}\right)_{at y=0} = -B_4 m_6 + A_3 m_2 + A_2 P_1 + \epsilon e^{nt} (-B_5 m_3 - A_4 m_6 + A_{10} m_2 + B_1 P_1 + B_2 m_5 + B_3 m_4) \quad (37)$$

$$Nu_x = x \frac{\left(\frac{\partial T}{\partial y^*}\right)_{at y=0}}{(T_w - T_\infty)} \Rightarrow Nu_x / Re_x = \left(\frac{\partial \theta}{\partial y}\right)_{at y=0} = (-m_2(1 - A_1) - A_1 P_1) + \epsilon e^{nt} (-m_5 A_9 - P_1 A_6 - m_2 A_7 - m_4 A_8) \quad (38)$$

$$Sh_x = x \frac{\left(\frac{\partial C}{\partial y^*}\right)_{at y=0}}{(C_w - C_\infty)} \Rightarrow Sh_x / Re_x = \left(\frac{\partial \phi}{\partial y}\right)_{at y=0} = -P_1 + \epsilon e^{nt} (-m_4(1 - A_5) - A_5 P_1) \quad (39)$$

where  $Re_x = \frac{V_0 x}{\nu}$  is the local Reynolds number.

#### 4. Results and discussion

The analytical solutions are performed for concentration, temperature and velocity for various values of fluid flow parameters such as Schmidt number  $Sc$ , chemical reaction parameter  $\gamma$ , Dufour number  $Du$ , Magnetic field parameter  $M$ , Heat absorption parameter  $\phi$ , Radiation absorption parameter  $Q_1$ , Radiation parameter  $F$ , Porous permeability parameter  $\phi_1$ , Porosity parameter  $K$ , Solutal Grashof number  $Gr$ , mass Grashof num  $Gm$  are presented in figures 1-16. Throughout the calculations the parametric values are chosen as  $Pr=0.71$ ,  $A=0.5$ ,  $\epsilon = 0.02$ ,  $n = 0.1$ , and  $t = 1$ .

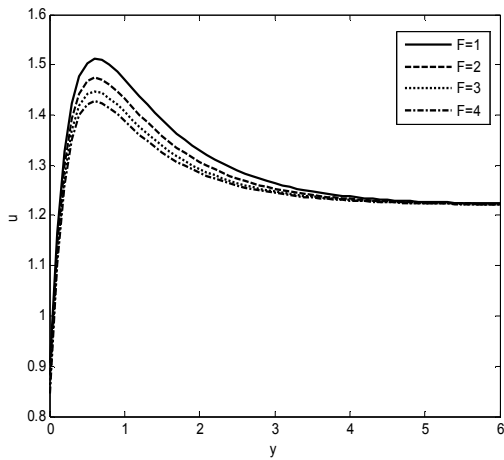


**Fig. 1.** Velocity profiles for various values of  $F$  with  $K = 0.1, Sc = 0.6, Gr = 4.0, Gm = 2.0, Q_1 = 2.0, \phi = 1, M = 2.0, Du = 0.5, \phi_1 = 0.3, \gamma = 0.5$ .

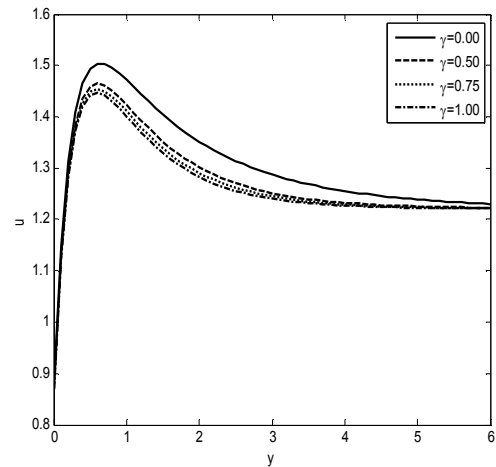


**Fig. 2.** Velocity profiles for various values of  $\gamma$  with  $K = 0.1, Sc = 0.6, Gr = 4.0, Gm = 2.0, Q_1 = 2.0, \phi = 1, M = 2.0, Du = 0.3, \phi_1 = 0.3, F = 2.0$ .

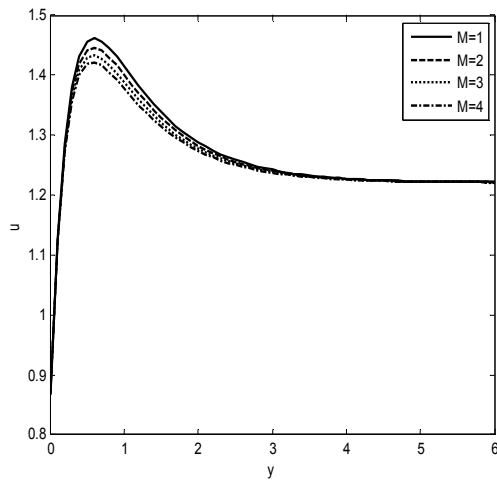


**Fig. 3.** Velocity profiles for various values of  $M$  with  $K = 0.1, Sc = 0.6, Gr = 4.0, Gm = 2.0, Q_1 = 2.0, \phi = 1.0, Du = 0.3, \phi_1 = 0.3, F = 2.0, \gamma = 1.$

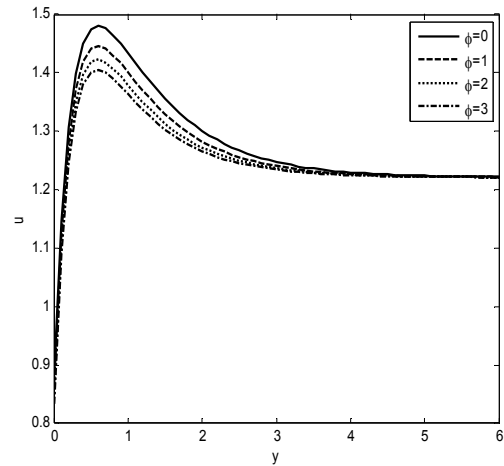


**Fig. 4.** Velocity profiles for various values of  $\phi$  with  $K = 0.1, Sc = 0.6, Gr = 4.0, Gm = 2.0, Q_1 = 2.0, Du = 0.3, \phi_1 = 0.3, F = 2.0, \gamma = 1, M = 2.$

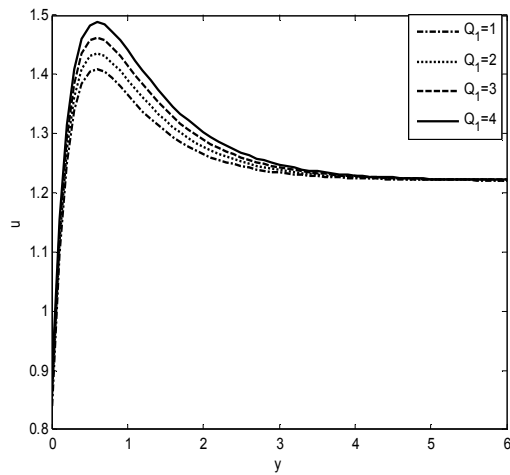


**Fig. 5.** Velocity profiles for various values of  $Q_1$  with  $K = 0.1, Sc = 0.6, Gr = 4.0, Gm = 2.0, M = 2.0, Du = 0.1, \phi_1 = 0.3, F = 2.0, \gamma = 1, \phi = 1.0.$

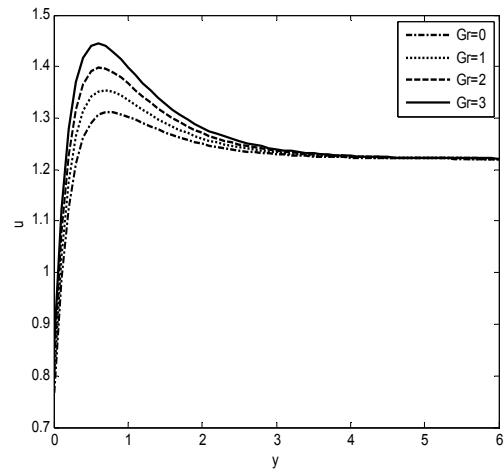


**Fig. 6.** Velocity profiles for various values of  $Gr$  with  $K = 0.1, Sc = 0.6, Gm = 3.0, M = 2.0, Q_1 = 2.0, Du = 0.3, \phi_1 = 0.3, F = 2.0, \gamma = 1, \phi = 1.0.$



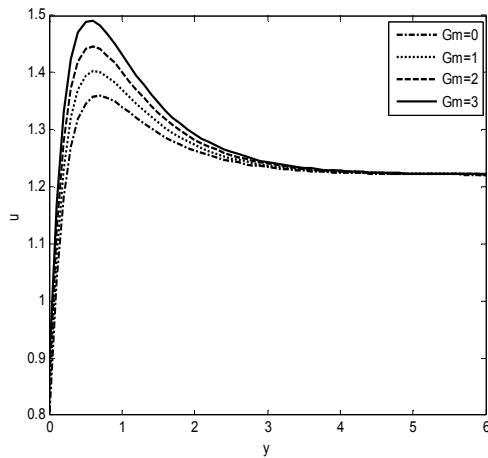


**Fig. 7.** Velocity profiles for various values of  $Gm$  with  $K = 0.1, Sc = 0.6, Gr = 4.0, M = 2.0, Q_1 = 2.0, Du = 0.3, \phi_1 = 0.3, F = 2.0, \gamma = 1, \phi = 1.0$ .

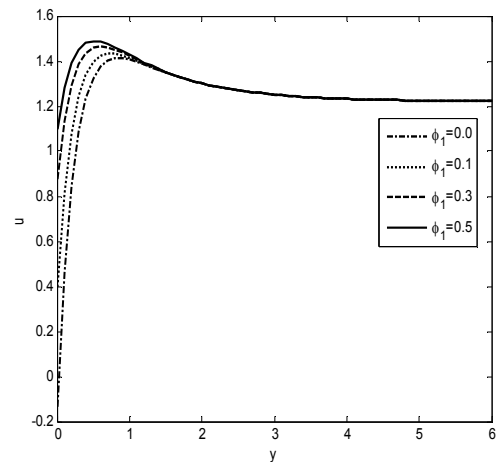


**Fig. 8.** Velocity profiles for various values of  $\phi_1$  with  $K = 0.1, Sc = 0.6, Gr = 4.0, Gm = 3.0, M = 2.0, Q_1 = 2.0, Du = 0.3, F = 2.0, \gamma = 0.5, \phi = 1.0$ .

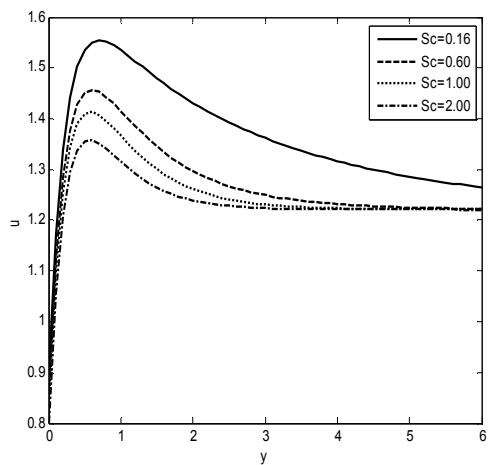


**Fig. 9.** Velocity profiles for various values of  $Sc$  with  $K = 0.1, Gr = 2.0, Gm = 2.0, M = 2.0, Q_1 = 2.0, Du = 0.1, \phi_1 = 0.3, F = 2.0, \gamma = 0.5, \phi = 1.0$ .

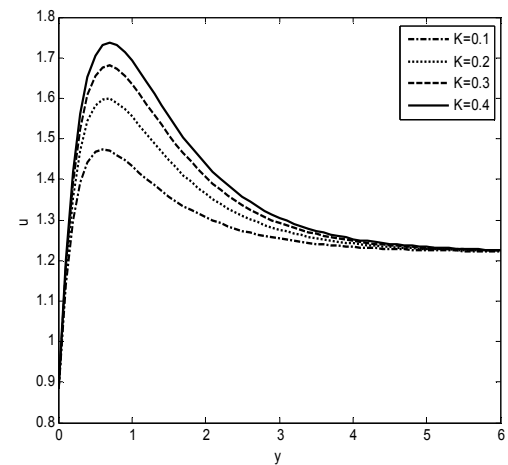


**Fig. 10.** Velocity profiles for various values  $K$  with  $Sc = 0.6, Gr = 4.0, Gm = 2.0, Q_1 = 2.0, Du = 0.5, \phi_1 = 0.3, F = 2.0, \phi = 1.0, \gamma = 0.5, M = 2.0$ .

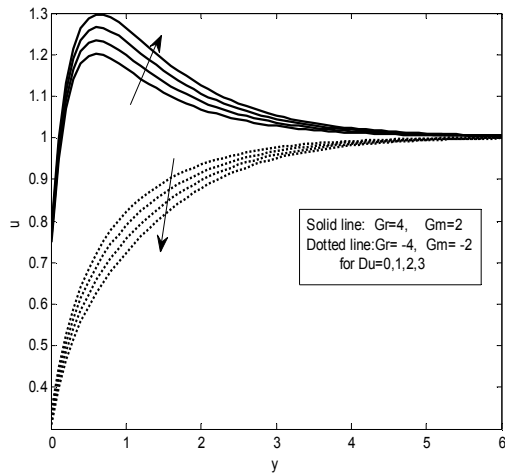


**Fig. 11.** Velocity profiles for various values  $Du$  with  $Sc = 0.6, Q_1 = 2.0, Du = 0.5, \phi_1 = 0.3, F = 2.0, \phi = 1.0, \gamma = 0.5, M = 2.0$ .

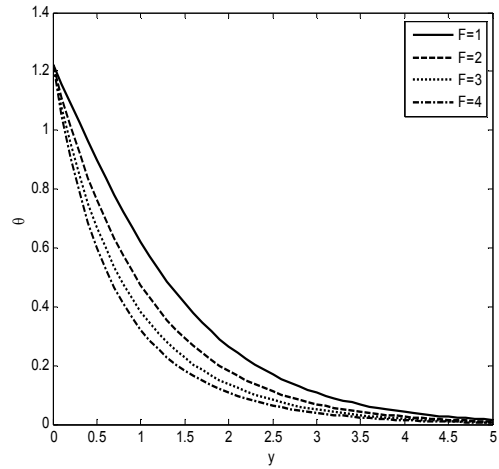


**Fig. 12.** Temperature profiles for various values of  $F$  with  $Sc = 0.6, Gr = 4.0, Gm = 3.0, M = 2.0, Q_1 = 2.0, Du = 0.5, \phi_1 = 0.3, \phi = 1.0$ .

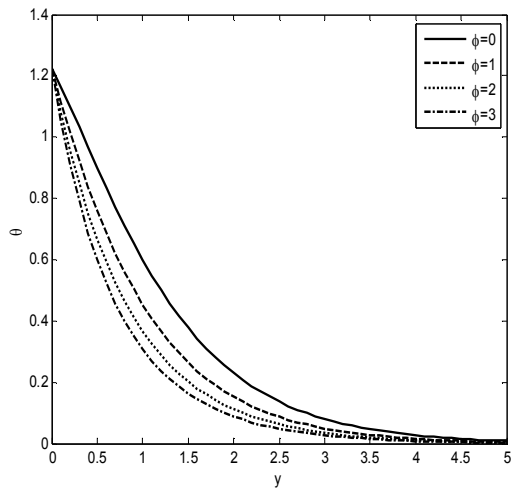


**Fig. 13.** Temperature profiles for various values of  $\phi$  with  $Sc = 0.6, Gr = 4.0, Gm = 3.0, M = 2.0, Q_1 = 2.0, Du = 0.5, \phi_1 = 0.3, F = 2.0, \gamma = 1.0$ .

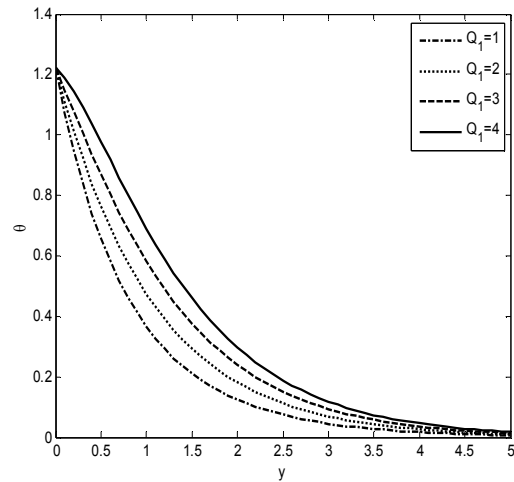


**Fig. 14.** Temperature profiles for various values of  $Q_1$  With  $Sc = 0.6, Gr = 4.0, Gm = 3.0, M = 2.0, Du = 0.5, F = 2.0, \phi = 1.0, \gamma = 0.5$ .

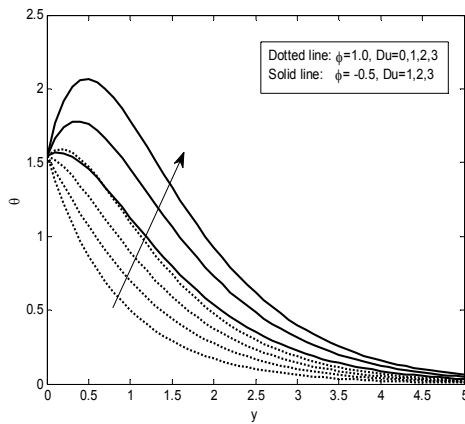


**Fig. 15.** Temperature profiles for various  $Du$  with  $Sc = 0.6, Q_1 = 2.0, F = 2.0, \gamma = 0.5$ .

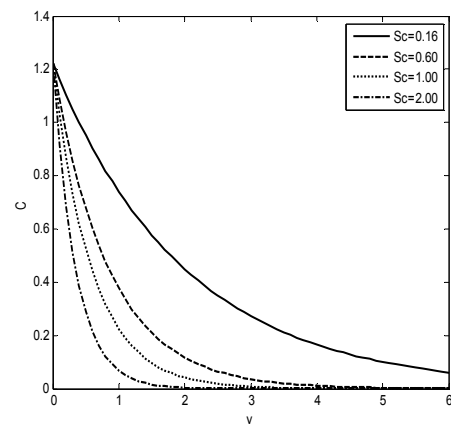


**Fig. 16.** Concentration profiles for various values of  $Sc$  with  $\gamma = 0.5$ .

**Table 1.** Comparing the present results with those of Kim [33] & Pal and Talukdar [6] with different values of  $C_{fx}$  and  $Nu_x/Re_x$ .

Kim[33] ( $G = 2, K = \infty, U_p = 0$ )			Pal and Talukdar [6] ( $Gr = 2, \phi = 0, \phi_1 = 0, F = 0,$ $K = \infty, Q_1 = 0, Gm = 0$ )			Present Results $Gr = 2, \phi = 0, \phi_1 = 0, F = 0, K =$ $\infty, Q_1 = 0, Gm = 0, Du = 0$		
$M$	$C_{fx}$	$Nu_x/Re_x$	$M$	$C_{fx}$	$Nu_x/Re_x$	$M$	$C_{fx}$	$Nu_x/Re_x$
0	4.5383	-0.9430	0	4.5383	-0.9430	0	4.5383	-0.9430
2	3.9234	-0.9430	2	3.9234	-0.9430	2	3.9234	-0.9430
5	4.4457	-0.9430	5	4.4457	-0.9430	5	4.4457	-0.9430
10	5.2976	-0.9430	10	5.2976	-0.9430	10	5.2976	-0.9430

**Table 2.** Comparison of present results with those of Pal and Talukdar [6] with different values of  $C_{fx}$ ,  $Nu_x/Re_x$  ( $F = 2, \phi = 1, M = 2, Q_1 = 2, Gr = 4, Gm = 2, Sc = 0.6, \phi_1 = 0.3$ ).

$\gamma$	$C_{fx}$	$Nu_x/Re_x$	$Sh_x/Re_x$	$C_{fx}$	$Nu_x/Re_x$	$Sh_x/Re_x$
	(Pal and Talukdar [6])			(Present results)		
0.0	4.0441	-1.3400	-0.8098	4.0442	-1.3400	-0.8098
0.50	3.7512	-1.4825	-1.1864	3.7513	-1.4825	-1.1864
0.75	3.6744	-1.5226	-1.3178	3.6744	-1.5227	-1.3178
1.00	3.6149	-1.5546	-1.4325	3.6149	-1.5546	-1.4326

**Table 3.** Effects of  $\phi_1$  ( $F = 2$ ) and  $F$  ( $\phi_1 = 0.3$ ) for fixed values of  $Gr = 4, Gm = 2, Sc = 0.6, M = 2, \phi = 1, Q_1 = 2, \gamma = 0.1, Du = 0.5, K = 0.5$

$\phi_1$	$C_{fx}$	$F$	$C_{fx}$	$Nu_x/Re_x$
0.0	6.2727	1.0	3.6557	-0.8319
0.1	4.9698	2.0	3.5111	-1.3014
0.3	3.5111	3.0	3.4129	-1.6742
0.5	2.7143	4.0	3.3400	-1.9860

**Table 4.** Effects of  $K$  ( $Du = 0.5$ ) and  $Du$  ( $K = 0.5$ ) for the constany values of  $Gr = 4, Gm = 2, Sc = 0.6, M = 2, \phi = 1, Q_1 = 2, \gamma = 0.1, \phi_1 = 0.3, F = 2$ .

$K$	$C_{fx}$	$Du$	$C_{fx}$	$Nu_x/Re_x$
1.0	3.7067	1.0	3.5631	-1.2245
2.0	3.8500	2.0	3.6671	-1.0667
3.0	3.9080	3.0	3.7712	-0.9089
4.0	3.9394	4.0	3.8752	-0.7512

The effect of radiation parameter  $F$  is shown in Fig. 1. It is observed in this figure that velocity profiles decrease with an increase in the radiation parameter  $F$ . Also, the increase of the radiation parameter leads to decrease in the momentum boundary layer thickness and reduces the heat transfer rate in the presence of thermal and solutal buoyancy forces. Figure 2 illustrates the effect of chemical reaction parameter  $\gamma$ . It is clear that, at first, the velocity increases and, later on, it decreases uniformly with the increasing values of  $\gamma$ . It is interesting to observe that the peak values of the velocity profiles are attained near the porous boundary surface. The velocity profiles for different values of magnetic parameter  $M$  are depicted in fig.3. From this figure it is clear that as the magnetic field parameter increases, the Lorentz force, which opposes the fluid flow also increases and leads to an enhance deceleration of the flow. This result qualitatively agrees with the expectations since the magnetic field exerts retarding force on the free convection flow. Fig.4 represents the fluid velocity decreases as the heat absorption parameter  $\phi$  increases and hence momentum boundary layer thickness decrease.

Figures 5 and 14 display the effects of the radiation absorption parameter  $Q_1$  on velocity and temperature fields. It is obvious from the figures that an increase in the absorption radiation parameter  $Q_1$  results in an increase in the velocity and temperature profiles within the boundary layer as well as an increase in the momentum and thermal thickness, because the large values of  $Q_1$  correspond to the increased domination of conduction over absorption

radiation, thereby increasing buoyancy force and thickness of the thermal and momentum boundary layers. According to Fig. 5, it is clear that velocity starts from the minimum value of zero at the surface and increases until reaching the peak value. Different values of the thermal buoyancy force parameter  $Gr$  and solutal buoyancy force parameter  $Gm$  are plotted in Figs. 6 and 7. As seen from the figures, maximum peak value is attained and minimum peak value is observed in the absence of buoyancy force, which is due to fact that buoyancy force enhances fluid velocity and increases the layer thickness with an increase in the value of  $Gr$  or  $Gm$ . Figure 8 illustrates the variation of velocity distribution across the boundary layer for various values of the porous permeability parameter  $\phi_1$ . It is observed that velocity increases near the source and reaches the free stream condition. Permeability  $\phi_1$  is directly proportional to the square root of the actual permeability  $K$ . Hence, an increase in  $\phi_1$  will decrease the resistance of the porous medium which will tend to accelerate the flow and increase the velocity.

The influence of Schmidt number  $Sc$  on the velocity profiles is shown in Fig. 9, in which at very low values of Schmidt number (e.g.  $Sc = 0.16$ ), there is an increase in the peak velocity near the plate ( $y \approx 1$ ), whereas for higher values of Schmidt number, the peak shifts closer to the plate. Further, it is observed that the momentum boundary layer decreases with an increase in the value of  $Sc$ . Figure 10 represents the influence of the porosity parameter  $K$  on velocity; maximum peak value is obtained for  $K = 0.4$  and minimum peak

value is observed for  $K = 0.1$ . Also it is clear that velocity increases significantly with the increasing values of  $K$ .

The temperature profiles for different values of the radiation parameter  $F$  are shown in Fig. 12. It is observed that an increase in the radiation parameter  $F$  results in a decrease in the thermal boundary layer thickness. Further, temperature is very high on the porous boundary and asymptotically decreases to zero as  $y \rightarrow \infty$ . Figure 13 depicts the variations in temperature profile against spanwise co-ordinate  $y$  for different values of heat absorption parameter  $\phi$ . From this figure, it is clearly understood that heat absorption parameter condenses the thickness of the temperature boundary layer, because when heat is absorbed, the buoyancy force decreases the temperature. The effect of Schmidt number  $Sc$  on the species concentration profiles is shown in Fig. 16. It is clear that the concentration decreases exponentially and reaches the free stream condition. Also, it is noticed that the concentration boundary layer thickness decreases with  $Sc$ .

The temperature profiles for different values of Dufour number in heat absorption ( $\phi > 0$ ) and heat generation ( $\phi < 0$ ) cases are shown in fig.15. It can be seen that the fluid temperature increases with Dufour number in both the cases. Thermal boundary layer thickness is higher in the case of heat absorption than that in the case of heat generation. Physically, the Dufour term that appears in the temperature equation measures the contribution of concentration gradient to thermal energy flux in the flow domain. It has a vital role in enhancing the flow velocity and the ability to increase the thermal energy in the boundary layer. As a result, the temperature profile at all time stages increases with the increase in  $Du$ .

Fig.11 displays the velocity profiles for various values Dufour number in the cases of cooling and heating of the plate. The velocity increases with Dufour number in the case of heating of the plate and opposite trend is observed in the case of cooling of the plate.

From Table.1 and Table.2, it is observed that the skin friction at the plate decreases with increasing chemical reaction parameter  $\gamma$  or

Magnetic parameter  $M$ . It is also noticed that the Nusselt number and Sherwood number decreases with increase in  $\gamma$ .

The influence of porous parameter  $\phi_1$  on Skin-friction, and radiation parameter  $F$  on skin-friction and Nusselt number are presented in Table. 3. It is observed that the skin friction at the plate decreases with increasing  $\phi_1$  or  $F$ . As the radiation parameter increases the heat is transferred from the plate to the fluid .

The effects of Permeability Parameter  $K$  on Skin-friction and Diffusion thermo parameter  $Du$  on Skin-friction and Nusselt number are presented in table.4. From this table it is obvious that the Skin friction and the Nusselt number increases with an increase in  $Du$ . It also clear that the Skin friction increases with the increasing values of  $K$ .

### 5. Comparison of the results

In order to examine the accuracy of the results of the present study, it is considered that the analytical solutions obtained by Kim [33], Pal and Talukdar[6] who computed the numerical results for Skin friction coefficient and Nusselt number. These computed and compared results are presented in Table.1. From this table it is interesting to observe that the present results in the absence of Diffusion-thermo effect and Porous medium are in good agreement with the corresponding results obtained from Pal and Talukdar [6]. It is also observed that the present results are in good agreement with those of Kim [33] when  $G = 2, K = \infty, u_p = 0, Du = 0, Gm = 0$ . Also from Table. 2, it is clear that the present results for skin-friction, Nusselt number and Sherwood number for different values of chemical reaction in the absence of porous medium and diffusion thermo effect are in good agreement with the corresponding results of Pal and Talukdar [6], which clearly shows the correctness of our present analytical solutions and computed results.

### 6. Conclusions

In this paper, we studied the Dufour effect on an unsteady MHD convective heat and mass transfer flow through a high porous medium

over a vertical porous plate. From the present study, the following conclusions can be drawn:

1. The diffusion-thermo parameter increases the thermal and momentum boundary layer thickness.
2. The fluid velocity increases with an increasing values of porous permeability parameter (slip parameter)  $\phi_1$ .
3. The Skin friction at the plate increases with an increasing values of  $Du$  or  $K$ .
4. The rate of heat transfer coefficient at the plate ( $Nu_x$ ) increase with Dufour number while it is decreases as chemical reaction parameter ( $\gamma$ ) or Radiation parameter ( $F$ ) increases.

### References

- [1] R. S. Rath, and D. N. Parida, "Magneto-hydrodynamic free convection in the boundary layer due to oscillation in the wall temperature", *Wear*, Vol. 78, No. 1, pp. 305-314, (1982).
- [2] A. Raptis, G. Tzivanidis, and N.Kafusias, "Free convection and mass transfer flow through a porous medium bounded by an infinite vertical limiting surface with constant suction", *Letters in Heat and Mass Transfer*, Vol. 8, No. 1, pp. 417-424, (1981).
- [3] B. K. Jha, and R. Prasad, "MHD free-convection and mass transfer flow through a porous medium with heat source", *Astrophysics and Space Science*, Vol. 18, No. 1, pp. 117-123, (1991).
- [4] K.Yamamoto, and N. Iwamura, "Flow with convective acceleration through a porous Medium", *J. Eng. Math*, Vol. 10, No. 1, pp .41-54, (1976).
- [5] B. Gebhart, and L. Pera, "The nature of vertical natural convection flows resulting from the combined buoyancy effects of thermal and mass diffusion", *Int. J. Heat and Mass Transfer*, Vol. 14, No. 12, pp. 2025-2050, (1971).
- [6] D. Pal and B. Talukdar, "Perturbation Analysis of unsteady magneto hydro -dynamic convective heat and mass transfer in a boundary layer slip flow past a vertical permeable plate with thermal radiation and chemical reaction", *Commun Nonlinear Sci Number Simulant*, Vol. 15, No. 7, pp. 1813-1830, (2010).
- [7] D. Nield and A. Bejan, "Convection in porous media", 2<sup>nd</sup> edition Springer, Wiley, New York, pp. 62-75, (1995).
- [8] P. Cheng, "Heat transfer in geothermal system", *Adv Heat Transfer*, Vol. 4, No. 1, pp. 1-105, (1978).
- [9] N. Rudraiah, "Flow through and past porous media, " *Encyclopedia of Fluid Mechanics*, Gulf Publ. Vol. 5, pp. 567-647, (1986).
- [10] N. Rudraiah, D. Pal, and I. N. Shivakumara, "Effect of slip and magnetic field on composite systems". *Fluid Dyn. Res.*, Vol. 4, No.4, pp. 255-270, (1988).
- [11] A. Apelblat, "Mass transfer with a chemical reaction of the first order: Analytical Solutions", *The Chemical Engineering Journal* Vol. 19, No. 1, pp. 19-37, (1980).
- [12] U. N. Das, R. K. Deka and V. M. Soundalgekar, "Effects of Mass transfer on flow past an impulsively started infinite vertical plate with constant heat flux and chemical reaction", *Forschung im Ingenieurwesen*, Vol. 60, No. 10, pp. 284-287, (1994).
- [13] P. L. Chambre and J. D. Young, "On the diffusion of a chemically reactive species in a laminar boundary layer flow", *The Physics of Fluids*, Vol. 1, pp. 48-54, (1958).
- [14] W. G. England, and A. F. Emery, "Thermal radiation effects on the laminar free convection boundary layer of an absorbing gas", *Journal of Heat Trans*, Vol. 91, No. 1, pp. 37-44, (1969).
- [15] V. M. Soundalgekar, and H. S. Takhar, "Radiation effects on free convection flow past a semi-vertical plate", *Modeling Measurement and Control*, Vol. 51, pp. 31-40, (1993).
- [16] A. Raptis, and C. Peridikis, "Radiation and free convection flow past a moving plate", *International Journal of Applied Mechanics and Engineering*, Vol. 4, No. 4, pp. 817-821, (1999).
- [17] F. S. Ibrahim, A. M. Elaiw and A. A. Bakr, "Effects of the chemical reaction

- and radiation absorption on the unsteady MHD free convection flow past a semi-infinite vertical permeable moving plate with heat source and suction”, *Communications in Nonlinear Science and Numerical Simulation*, Vol. 13, No. 6, pp. 1056-1066, (2008).
- [18] Z. Dursunkaya, and W. M. Worek, “Diffusion–thermo and thermal-diffusion effects in transient and steady natural convection from vertical surface”, *International Journal of Heat and Mass Transfer*, Vol. 35, No. 8, pp. 2060-2065, (1992).
- [19] M. Anghel, H. S. Takhar and I. Pop, “Dufour and Soret effects on free convection boundary layer over a vertical surface embedded in a porous medium”, *Studia Universitatis Babeş-Bolyai, Mathematica* Vol. 45, No. 4, pp. 11-21, (2000).
- [20] A. Postelnicu, “Influence of a magnetic field on heat and mass transfer by natural convection from vertical surfaces in porous media considering Soret and Dufou effects”, *International Journal of Heat and Mass Transfer*, Vol. 47, No. 6, pp. 1467-1472, (2004).
- [21] A. J. Chamkha, “Unsteady MHD convective heat and mass transfer past a semi-infinite vertical permeable moving plate with heat absorption”, *International Journal of Engineering Sciences*, Vol. 42, No. 2, pp. 217-230, (2004).
- [22] A. J. Chamkha, “MHD flow of a uniformly stretched vertical permeable surface in the presence of heat generation/absorption and a chemical reaction”, *Int. Comm. Heat Mass Transfer*, Vol. 30, No. 3, pp. 413-422, (2003).
- [23] R. A. Mohamed, “Double-diffusive convection radiation interaction on unsteady MHD flow over a vertical moving porous plate with heat generation and Soret effects”, *Appl. Math. Sci.*, Vol. 3, No. 13, pp. 629-651, (2009).
- [24] R. Muthucumaraswamy and B. Janakiraman, “MHD and radiation effects on moving isothermal vertical plate with variable mass diffusion”, *Theo. Appl. Mech.*, Vol. 33, No.1, pp. 17-29, (2006).
- [25] V. Rajesh and S. V. K. Varma, “Thermal diffusion and radiation effects on MHD flow past an impulsively started infinite vertical plate with variable temperature and mass diffusion”, *JP J. Heat and Mass Transfer*, Vol. 3, No. 1, pp. 17-39, (2009).
- [26] A. G. Vijaya Kumar and S. V. K. Varma, “Thermal radiation and mass transfer effects on MHD flow past an impulsively started exponentially accelerated vertical plate with variable temperature and mass diffusion”, *Far East J. Appl. Math.*, Vol. 55, No. 2, pp. 93-115, (2011).
- [27] R. A. Raptis, C. Perdikis and A. Leontitsis, “Effects of radiation in an optically thin gray gas flowing past a vertical infinite plate in the presence of magnetic field”, *Heat and Mass Transfer*, Vol. 39, pp. 771-773, (2003).
- [28] A. Orhan and K. Ahmad, “Radiation effect on MHD mixed convection flow about a permeable vertical plate”, *Heat and Mass Transfer*, Vol. 45, No. 2, pp. 239-246, (2008).
- [29] S. Ahmad, “Inclined magnetic field with radiating fluid over a porous vertical plate: Analytical study”, *Journal Naval Arch. Marine Engineering*, Vol. 7, No. 2, pp. 61-72, (2010).
- [30] E. R. G. Eckert, and R. M. Drake, “Analysis of Heat and Mass Transfer”, *M.C.Graw-Hill*, New- York, (1972).
- [31] J. Prakash, D. Bhanumathi, A. G. Vijaya Kumar “Radiation effects on unsteady MHD flow through porous medium past an impulsively started infinite vertical plate with variable temperature and mass diffusion”, *Trans. Porous Med.* Vol. 96, No. 1, pp. 135-151, (2013).
- [32] A. C. Cogley, W. G. Vincent and S. E. Giles, “Differential approximation to radiative heat transfer in a non-grey gas near equilibrium”, *American Institute of Aeronautics and Astronautics*, Vol. 6, No. 3, pp. 551-553, (1968).

- [33] Y. J. Kim, “Unsteady MHD convective heat transfer past a semi-infinite vertical moving plate with variable suction”,

*International Journal of Engineering Sciences*, Vol. 38, No. 8, pp. 833-845, (2000).